

On the significance of relativistically hot pairs in the jets of FR II radio galaxies

Marek Sikora,^{1*} Krzysztof Nalewajko,^{1†} Greg M. Madejski,²

¹*Nicolaus Copernicus Astronomical Center, Polish Academy of Sciences, Bartycka 18, 00-716 Warsaw, Poland*

²*Kavli Institute for Particle Astrophysics and Cosmology, Stanford University, Stanford, CA 94305, USA*

30 April 2022

ABSTRACT

The energetic composition of radio lobes in the FR II galaxies — estimated by comparing their radio luminosities with the powers required to inflate cavities in the external medium — seems to exclude the possibility of their energetic domination by protons. Furthermore, if the jets were dominated by the kinetic energy of cold protons, it would be difficult to efficiently accelerate leptons in the jets’ terminal shocks. This suggests that the jets powering the lobes are dominated by pairs not only in number but also in enthalpy. Such a possibility is confronted against the constraints imposed by the jet formation scenarios, and by the properties of jets on parsec and kiloparsec scales. We find a lower limit on the pair content from the energetic dominance of leptons over protons in the radio lobes, which exceeds the estimate of $n_e/n_p \sim 20$ indicated by models of the blazar zones and of the radio cores. This allows us to establish that the average energy of protons in the jet co-moving frame is $< 2m_p c^2$, and to estimate the number fluxes of protons and e^+e^- pairs. The required proton flux is achievable, if the jet carries away about 1% of the accreting matter. Loading the jets by pairs can be achieved by pair creation using soft γ -ray photons from the accretion disk corona, provided that about 2-3% of the disk radiation extends beyond 1 MeV. Finally, we discuss possible dissipative mechanisms which may keep the jets dominated by relativistically hot pairs.

Key words: quasars — galaxies: active — galaxies: jets — radiation mechanisms: non-thermal — acceleration of particles

1 INTRODUCTION

Calorimetry of luminous radio lobes associated with some radio galaxies and quasars indicates that they must be powered at the rates corresponding with their AGN accretion powers (e.g., Rawlings, & Saunders 1991; Punsly 2007; Fernandes et al. 2011; Rusinek et al. 2017). Such energy is transmitted from AGNs to radio lobes by relativistic jets. These jets have been observed in many spectral bands (radio, infrared, optical, X-ray) on distance scales ranging from sub-parsecs up to hundreds of kiloparsecs (see the review by Blandford et al. 2019). Despite steady progress in the multi-band coverage, sensitivity and angular resolution of these observations, the physical structure of jets, and its dependence on the distance from the central black hole (BH), remain unclear. The main reasons for this are: (1) a rather weak dependence of the morphology of radio lobes on the matter content and magnetisation of the underlying jets (e.g.,

Mignone et al. 2010); (2) a variety of dissipation mechanisms which can lead to similar radiative properties of jets (e.g., Blandford et al. 2019, and refs. therein); (3) an unknown efficiency of loading jets by mass (e.g., O’ Riordan et al. 2018); (4) a poor observational knowledge of the jets lateral structure (e.g., Perlman et al. 2019).

Relativistic speeds and powers of jets in luminous radio galaxies and quasars associated with the FR II radio sources (Fanaroff & Riley 1974) seem to support the production of jets by the Blandford-Znajek mechanism (Blandford & Znajek 1977) involving Magnetically Arrested Disks (MAD; Narayan et al. 2003; Punsly et al. 2009; McKinney et al. 2012). In such a case, the magnetic flux threading the BH is maximised, and the rate at which the rotational energy of rapidly rotating BHs can be extracted and converted by magnetic stresses to the kinetic energy of the outflows can reach or even exceed the accretion power (Tchekhovskoy et al. 2011). Such outflows are initially dominated by the Poynting flux, but within $\sim 2 - 4$ distance decades about half of this flux is theoretically predicted to be converted to the kinetic energy of cold protons (Begelman & Li 1994;

* E-mail: sikora@camk.edu.pl

† E-mail: knalew@camk.edu.pl

Lyubarsky 2010). One might try to verify this by studying blazars, which emit most of their beamed radiation just at these distances (e.g., Nalewajko et al. 2014; Janiak et al. 2015).

The observed spectral energy distributions (SED) of blazars can be in most cases reproduced by either the so-called ‘leptonic’ models or the ‘(lepto)-hadronic’ models (Böttcher et al. 2013). The main difference is that, since the radiative efficiency of energetic protons is systematically lower than that of electrons/positrons (Sikora et al. 2009), hadronic models require minimum jet powers larger typically by a factor ~ 100 . In many cases (especially for the more luminous flat spectrum radio quasars, FSRQs, associated with the FR II radio sources) the hadronic jet power would exceed the Eddington luminosity corresponding to given BH mass (Zdziarski, & Böttcher 2015), but also the accretion disk power that can be constrained independently from the luminosity of the broad emission lines. However, even for the strictly leptonic SED models, and even in the limit of completely cold protons, the contribution of protons to the total jet power can be dominant, provided that $\bar{\gamma}_e < (n_p/n_e)(m_p/m_e)$, where $n_e = (n_{e+}) + (n_{e-})$. In the case of no pairs ($n_p = n_e$), the powers of blazar jets calculated by Ghisellini et al. (2014) are found to exceed by a factor ~ 20 the jet powers estimated using the calorimetry of radio lobes (Kang et al. 2014; Sikora 2016; Pjanka et al. 2017; Fan et al. 2018) and radio core shifts studies (Pjanka et al. 2017).

Little information on the proton content is available from the studies of radiative spectra of the large-scale jets, or from the radio lobes. Relativistic jets are considered as candidate sites for production of ultra-high-energy cosmic rays (UHECR) (e.g., Murase et al. 2014; Rodrigues et al. 2018), and it has been suggested that synchrotron emission of ultra-relativistic protons may explain the extended X-ray emission from kpc-scale jets (e.g., Aharonian 2002). However, as we argue below, the vast majority of protons in relativistic jets should be sub-relativistic, and as such they would yield no observational signatures that could be directly detected.

One might try to recover information about the proton content by studying the rates at which matter can entrain the jet at its base via interchange instabilities. However, because the jets are formed as strongly electromagnetically dominated outflows, the efficiency of the proton loading cannot be self-consistently estimated using the currently available general relativistic MHD numerical simulations (O’Riordan et al. 2018). Jets can also be entrained by protons on larger distances, as a result of their interactions with the external medium (Chatterjee et al. 2019), or intrinsically – by winds of stars enclosed within the jet volume (Komissarov 1994; Perucho et al. 2014). While the dynamical effects of jet loading by stellar winds are likely to be important in case of low-power FR I radio galaxies (RGs), in the case of powerful jets in FR II RGs and quasars they are expected to be negligible (Perucho 2019).

We have a clearer picture for the problem of loading jets by electron-positron pairs. They can be created within the volume of the jet base by γ -rays emitted in high temperature accretion disk coronae (e.g., Beloborodov 1999). As it will be shown in this paper, the rate of pair creation required to provide the number flux of pairs needed to ex-

plain the blazar radiation and the leptonic energy content of radio lobes is achievable for reasonable parameters of accretion flows. However, as we already pointed out before, even for the pair-dominated jets, in the sense that the number density of pairs exceeds the number density of protons, one can still have the jet power dominated by the kinetic energy of cold protons. But this seems to be challenged by studies of luminous FR II radio sources showing that the energy content of radio lobes is likely to be dominated by the pairs (Kino et al. 2012; Kawakatu et al. 2016; Ineson et al. 2017; Snios et al. 2018; Turner et al. 2018; Croston et al. 2018). One could argue that the jet powers may still be dominated by the kinetic energy of cold protons by postulating that the kinetic energy of protons dissipated at the terminal shocks is roughly evenly redistributed between protons and pairs. However, the results of particle-in-cell (PIC) numerical simulations of relativistic shocks suggest that this would be possible only in the case of parallel shocks (with magnetic field lines parallel to the shock normal), while terminal shocks associated with the hot spots in radio lobes are expected to be perpendicular (see Sironi & Spitkovsky 2011; Crumley et al. 2019, and refs. therein).

This motivated us to investigate a scenario in which the large-scale relativistic jets are energetically dominated not by the cold protons, but rather by the hot and relativistic pair plasma (Snios et al. 2018). In §2 we derive the parameters of such jets using the observational data and theoretical constraints imposed by the studies of radio lobes and blazars; in §3 we check whether and how the hot, pair-dominated jets can be formed; and in the discussion section §4 we consider possible mechanisms which in the FR II objects could maintain the energy flux of the hot leptons at the level of (or slightly exceeding) the energy flux of the protons, and why it is not the case in the FR I objects. The main results of our study are summarised in §5.

2 THE STRUCTURE OF LARGE-SCALE RELATIVISTIC JETS

2.1 Energetic structure

Assuming that redistribution of energy between protons, electrons and magnetic fields at the jet terminal shocks is negligible – which we expect to be the case when the jet power is dominated by the internal energy flux – the ratio of electron to proton energy fluxes in the jet is

$$\frac{P_{e,\text{jet}}}{P_{p,\text{jet}}} \equiv \kappa_{e,\text{jet}} \simeq \kappa_{e,\text{lobe}} \equiv \frac{E_{e,\text{lobe}}}{E_{p,\text{lobe}}}, \quad (1)$$

and the magnetisation of the jet plasma is

$$\sigma_{\text{jet}} \equiv \frac{P_{B,\text{jet}}}{P_{e,\text{jet}} + P_{p,\text{jet}}} \simeq \frac{E_{B,\text{lobe}}}{E_{e,\text{lobe}} + E_{p,\text{lobe}}} = \frac{\sigma_{e,\text{lobe}} \kappa_{e,\text{lobe}}}{1 + \kappa_{e,\text{lobe}}}, \quad (2)$$

where $\sigma_{e,\text{lobe}} \equiv E_{B,\text{lobe}}/E_{e,\text{lobe}} \sim 0.3$ and $\kappa_{e,\text{lobe}} \gtrsim 1$, as determined from the radio and X-ray observations of the radio lobes and their environment in FR II sources (e.g., Kataoka, & Stawarz 2005; Croston et al. 2005; Ineson et al. 2017; Turner et al. 2018; Croston et al. 2018).

Neglecting the energy redistribution at the terminal shocks implies also that the average electron energy in the jet is $\bar{\gamma}_{e,\text{jet}} \sim \bar{\gamma}_{e,\text{hs}}/\Gamma_{\text{jet}}$, where $\bar{\gamma}_{e,\text{hs}} \sim 10^3$ is the average

energy of electrons in the hot spots (e.g., Carilli et al. 1991; Tavecchio et al. 2005; Stawarz et al. 2007; Godfrey et al. 2009; Turner et al. 2018; Harris et al. 2019), and Γ_{jet} is the jet Lorentz factor. One can then estimate the average energy of jet electrons as $\bar{\gamma}_{e,\text{jet}} \sim 100(\bar{\gamma}_{e,\text{hs}}/10^3)/(\Gamma_{\text{jet}}/10)$, hence, the leptonic jet plasma component is relativistically hot. Noting that $\kappa_{e,\text{jet}} = P_{e,\text{jet}}/P_{p,\text{jet}} = w_{e,\text{jet}}/w_{p,\text{jet}}$, where $w_i = n_i m_i c^2 [1 + \iota_i (\bar{\gamma}_i - 1)]$ are the enthalpy densities of the respective plasma components with adiabatic indices $\iota_p \geq \iota_e = 4/3$, we can estimate the minimum pair content of the jet plasma in the limit of cold protons ($\bar{\gamma}_i \rightarrow 1$):

$$\left(\frac{n_e}{n_p}\right)_{\text{min}} = \frac{3}{4} \left(\frac{m_p}{m_e}\right) \left(\frac{\kappa_{e,\text{jet}}}{\bar{\gamma}_{e,\text{jet}}}\right) \simeq 14 \left(\frac{100}{\bar{\gamma}_{e,\text{jet}}}\right) \kappa_{e,\text{jet}}. \quad (3)$$

This is comparable with an independent estimate of $n_e/n_p \sim 20$ based on the models of blazar emission and radio core shifts (e.g., Pjanka et al. 2017). From the above, one can also find that the average energy of jet protons is

$$\bar{\gamma}_{p,\text{jet}} \simeq \frac{\iota_p - 1}{\iota_p} + \frac{1}{\kappa_{e,\text{jet}}} \left(\frac{\iota_e}{\iota_p}\right) \left(\frac{n_e/n_p}{20}\right) \left(\frac{\bar{\gamma}_{e,\text{jet}}}{100}\right). \quad (4)$$

From this one can conclude that the jet proton plasma is sub-relativistic ($\bar{\gamma}_{p,\text{jet}} < 2$).

2.2 Particle number fluxes

Calorimetry of the radio lobes, combined with the models of their time evolution, allows one to estimate the total jet power (e.g., Rawlings, & Saunders 1991; Willott et al. 1999; Cavagnolo et al. 2010; Godfrey, & Shabala 2013; Shabala, & Godfrey 2013; Hardcastle 2018). Considering the contributions from protons, electrons and magnetic fields, we have $P_{\text{jet}} = P_{p,\text{jet}} + P_{e,\text{jet}} + P_{B,\text{jet}}$. With the aforementioned estimates of $\kappa_{e,\text{jet}} \simeq \kappa_{e,\text{lobe}}$, one can find that

$$P_{e,\text{jet}} = \left(\frac{\kappa_{e,\text{jet}}}{1 + \kappa_{e,\text{jet}}}\right) \frac{P_{\text{jet}}}{1 + \sigma_{\text{jet}}}, \quad (5)$$

and then use Eqs. (1) and (2) to evaluate $P_{p,\text{jet}}$ and $P_{B,\text{jet}}$.

Since $\bar{\gamma}_{e,\text{jet}} \gg 1$, the leptonic component of the jet power can be expressed in the form

$$P_{e,\text{jet}} \simeq (4/3) \Gamma_{\text{jet}} \bar{\gamma}_{e,\text{jet}} m_e c^2 \dot{N}_{e,\text{jet}}, \quad (6)$$

where $\dot{N}_{e,\text{jet}}$ is the electron number flux across the jet. Using this, we obtain

$$\dot{N}_{e,\text{jet}} = \left(\frac{\kappa_{e,\text{jet}}}{1 + \kappa_{e,\text{jet}}}\right) \frac{P_{\text{jet}}}{(4/3)(1 + \sigma_{\text{jet}}) \Gamma_{\text{jet}} \bar{\gamma}_{e,\text{jet}} m_e c^2}, \quad (7)$$

and $\dot{N}_{p,\text{jet}} = (n_p/n_e) \dot{N}_{e,\text{jet}}$.

3 MAKING THE HOT PAIR-DOMINATED RELATIVISTIC JETS

Both observations and theoretical models indicate that AGN jets are at all scales shaped by the pressure balance with their external environment. At the smallest scales they are presumably confined by the MHD winds from the accretion disk and take a parabolic shape (e.g., Bogovalov, & Tsinganos 2005; Beskin, & Nokhrina 2006; Zakamska et al. 2008; Lyubarsky 2010). On the kiloparsec scales, i.e., within the cores of their host galaxies, confinement is provided

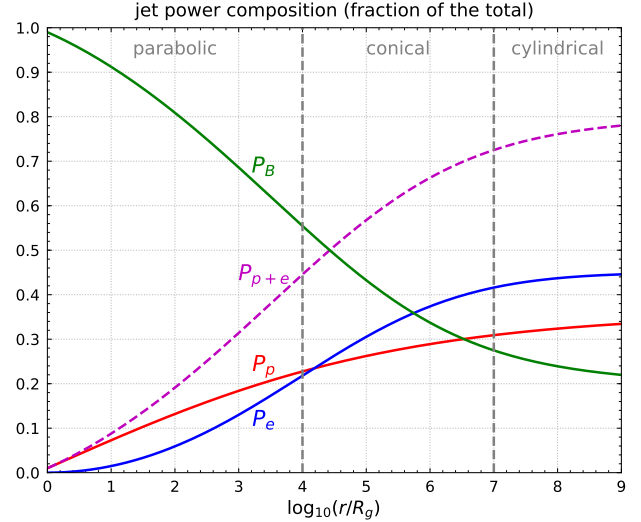


Figure 1. Suggested qualitative composition of the jet power as function of distance along the jet. Radiative energy losses are not included. We indicate the three main geometric jet zones.

by the interstellar medium (ISM). In that case, if the external pressure p_{ext} decreases with distance r faster than $p_{\text{ext}} \propto r^{-2}$, the jets would become conical (e.g., Falle 1991; Komissarov 1994; Lyubarsky 2009; Barniol Duran et al. 2017). Finally, outside the galaxies confinement would be provided by the roughly uniform pressure of the cocoon inflated by the shocked jet matter backflowing sideways from the jet terminal shock and the jets would become roughly cylindrical (e.g., Bromberg et al. 2011; Tchekhovskoy, & Bromberg 2016). In this ‘cylindrical zone’ of a jet, its intrinsic properties are expected to be independent of distance (no heating by dissipative processes associated with pressure matching of expanding flows; no adiabatic cooling; negligible radiative losses), and hence these parameters should be settled in the previous zones. Figure 1 illustrates schematically our suggested scenario for the composition of jet power evolving along multiple distance scales.

3.1 Mass loading of jets

The Blandford-Znajek mechanism of energy extraction from rotating black holes is an electromagnetic phenomenon, and therefore production of the jets requires loading of the Poynting-flux-dominated outflows with matter. In order for the jets to become relativistic, it is required that the mass loading rate \dot{M}_{load} should satisfy the condition $\dot{M}_{\text{load}} c^2 \ll P_{\text{jet}}$. Mass loading of relativistic jets is still poorly understood. One question is, where does it occur, whether at the jet base or at larger distances? Another question is, how does it happen? Because we anticipate different numbers of leptons and protons ($n_e/n_p \sim 20$), these questions will be considered separately for the pairs and for the protons.

Noting that jets powered by the Blandford-Znajek mechanism are launched as electromagnetic outflows with globally ordered poloidal magnetic field structures, and that the Larmor radii of non-relativistic protons is trillions of times lower than the lateral size of the outflow, the entrain-

ment of jets by protons from the disk and/or its corona is almost completely blocked (e.g. [Vila et al. 2014](#), and refs. therein). Numerical GRMHD simulations of the MADs indicate that the best candidate for loading the outflows by baryons might be the magnetic interchange instability (see [McKinney et al. 2012](#), and refs. therein). For loading jets by electron-positron pairs in AGN characterised by high and moderate accretion rates, we consider pair creation by γ -rays emitted in the coronae of hot accretion flows. Both mechanisms are very challenging for computational evaluation of their efficiencies. In the case of interchange instabilities, the difficulty comes from the limitations of direct MHD simulations in terms of resolving the MADs in 3D, as well as in an accurate treatment of magnetically dominated plasmas ([O’ Riordan et al. 2018](#)). In the case of pair creation, the main difficulty comes from the unknown AGN spectra in the soft γ -ray band extending beyond 1 MeV (e.g., [Gondek et al. 1996](#)). However, with the constraints on matter composition available on much larger scales, and assuming how they correspond to conditions at much smaller scales, we can at least try to verify whether the conditions required by these mechanisms to produce the necessary particle fluxes are feasible.

3.1.1 Pair Loading

The injection rate of electron-positron pairs due to the photon-photon annihilation within the jet base can be estimated as

$$\dot{N}_{e(\gamma\gamma)} = 2f_{\text{jb}}\dot{N}_{\gamma(>\text{MeV})}\tau_{\gamma\gamma}, \quad (8)$$

where f_{jb} is the fraction the total number of pairs produced by the AGN that are created within the volume occupied by the jet base, $\dot{N}_{\gamma(>\text{MeV})}$ is the emission rate of the $E > 1$ MeV photons by the hot accretion flow or its corona, and $\tau_{\gamma\gamma}$ is the absorption probability of these photons due to the pair production process. Using approximate formulae

$$\dot{N}_{\gamma(>\text{MeV})} \simeq \frac{f_{\gamma(>\text{MeV})}L_{\text{acc}}}{m_e c^2}, \quad (9)$$

$$\tau_{\gamma\gamma} \simeq n_{\gamma(>\text{MeV})}R_{\gamma}\sigma_{\gamma\gamma} \simeq \frac{f_{\gamma(>\text{MeV})}L_{\text{acc}}\sigma_{\gamma\gamma}}{4\pi R_{\gamma}m_e c^3}, \quad (10)$$

where L_{acc} is the bolometric luminosity of the accretion flow, $f_{\gamma(>\text{MeV})}$ is the fraction of that luminosity contained in the $E > 1$ MeV photons, R_{γ} is the approximate size of the region from which most of the γ -rays are emitted, $n_{\gamma(>\text{MeV})}$ is the mean number density of the $E > 1$ MeV photons within R_{γ} , and $\sigma_{\gamma\gamma}$ is the cross-section for the pair production process, we obtain

$$\begin{aligned} \dot{N}_{e(\gamma\gamma)} &\simeq f_{\text{jb}}f_{\gamma(>\text{MeV})}^2 \frac{\sigma_{\gamma\gamma}}{2\pi c R_{\gamma}} \left(\frac{L_{\text{acc}}}{m_e c^2} \right)^2 \\ &\simeq 2f_{\text{jb}}f_{\gamma(>\text{MeV})}^2 \frac{m_p}{m_e} \frac{\sigma_{\gamma\gamma}}{\sigma_T} \frac{\lambda_{\text{Edd}}}{(R_{\gamma}/R_g)} \frac{L_{\text{acc}}}{m_e c^2}, \end{aligned} \quad (11)$$

where $\lambda_{\text{Edd}} \equiv L_{\text{acc}}/L_{\text{Edd}}$ is the Eddington ratio, with $L_{\text{Edd}} = 4\pi m_p c^3 R_g / \sigma_T$ the Eddington luminosity, with $R_g = GM_{\text{BH}}/c^2$ the gravitational radius for BH mass M_{BH} , and σ_T the Thomson cross section. Hence, in order to load the jet by electrons at a rate $\dot{N}_{e,\text{jet}}$ (Eq. 7), the fraction of the accretion luminosity emitted at energies $E > 1$ MeV should

be

$$f_{\gamma(>\text{MeV})} \simeq 0.032 \left[\frac{(P_{\text{jet}}/L_{\text{acc}})(R_{\gamma}/10R_g)}{(f_{\text{jb}}/0.1)(\lambda_{\text{Edd}}/0.1)(\bar{\gamma}_{e,\text{hs}}/10^3)} \times \frac{\kappa_{e,\text{jet}}(1 + \sigma_{e,\text{jet}})}{(1 + \kappa_{e,\text{jet}})} \right]^{\frac{1}{2}}. \quad (12)$$

where $\sigma_{\gamma\gamma} \simeq 0.2\sigma_T$, and we adopt $\kappa_{e,\text{jet}} \simeq 1$, $\sigma_{e,\text{jet}} \simeq 0.3$ (see §2.1). This result cannot be directly verified by observations because of the very poor constraints on the AGN spectra in the soft γ -ray band (e.g., [Gondek et al. 1996](#)). The results from the Swift/BAT and INTEGRAL instruments show that the hard X-ray spectra in radio-loud AGN are characterised by photon indices < 2 , extending at least up to tens of keV (see [Burlon et al. 2013](#); [Panessa et al. 2015](#); [Bassani et al. 2016](#); [Ricci et al. 2017](#); [Gupta et al. 2018](#), and refs. therein). In some of these sources a high-energy break is indicated. However, without evidence for an exponential cut-off in those spectra, it cannot be excluded that a fraction of a few percent of the L_{acc} luminosity is emitted at photon energies above 1 MeV.

3.1.2 Proton loading

The required proton loading rate of the jet $\dot{M}_{p,\text{load}} \simeq P_{p,\text{jet}}/(\Gamma_{\text{jet}}c^2)$ can be estimated using Eqs. (1) and (5):

$$\dot{M}_{p,\text{load}} \simeq \frac{P_{\text{jet}}}{c^2 \Gamma_{\text{jet}}(1 + \kappa_{e,\text{jet}})(1 + \sigma_{\text{jet}})}. \quad (13)$$

Comparing this with the mass accretion rate $\dot{M}_{\text{acc}} = L_{\text{acc}}/(\epsilon_{\text{acc}}c^2)$, with ϵ_{acc} the radiative efficiency of the accretion flow, we estimate the proton loading efficiency as

$$\frac{\dot{M}_{p,\text{load}}}{\dot{M}_{\text{acc}}} \simeq 10^{-2} \frac{(\epsilon_{\text{acc}}/0.1)}{(\Gamma_{\text{jet}}/10)(1 + \kappa_{e,\text{jet}})(1 + \sigma_{\text{jet}})} \frac{P_{\text{jet}}}{L_{\text{acc}}}. \quad (14)$$

Whether such a rate of proton loading can be provided by the interchange instabilities, which drive the accretion onto BH in the MAD scenario, remains unclear ([O’ Riordan et al. 2018](#)). According to [Chatterjee et al. \(2019\)](#), who performed axisymmetric GRMHD numerical simulations of relativistic jets, significant mass loading can be obtained via a pinch mode of the interaction of a jet with its external medium. Jets could also be loaded by baryonic matter ‘intrinsically’, e.g., by the winds of stars enclosed within the jet volume, however, in the FR II jets the efficiency of such mechanism would be much lower than that required by Eq. (14) ([Komisarov 1994](#); [Perucho et al. 2014](#)).

3.2 Heating and cooling

Extremely high apparent luminosities of blazars (e.g., [Abdo et al. 2011](#); [Ackermann et al. 2016](#)), even considering their enhancement by relativistic effects, provide a strong evidence for very efficient dissipative processes responsible for particle heating and acceleration (see, e.g., [Madejski & Sikora 2016](#)). The observed variability time scales indicate that most of their radiation is emitted within $10^3 - 10^5 R_g$ (e.g., [Nalewajko et al. 2014](#)), i.e., by the end of the ‘parabolic zone’. This, however, does not prove that the dissipative processes work efficiently only at such distances. At smaller distances, the jets are not yet expected to be well accelerated and collimated, therefore any radiation produced there

is beamed much less strongly, and as such it would not contribute much to the radiation observed in blazars. In turn, at larger distances, those corresponding with the ‘conical zone’, the radiative signatures of dissipative processes can be very weak, because even for ultra-relativistic electrons the efficiency of radiative cooling becomes lower than that of their adiabatic losses (Sikora et al. 2013; Janiak et al. 2015). In a laterally expanding jet, if at some distance the dissipative processes would cease, the internal plasma energy would be spent on bulk acceleration, resulting in a ballistically propagating cold jet (Blandford et al. 2019, and refs. therein). However, if the dissipative processes do not cease, the continuous heating could at least partially compensate the adiabatic losses, and the jet plasma would remain relativistically hot (see Potter, & Cotter 2015; Zdziarski et al. 2019, and refs. therein).

Several dissipative processes have been proposed to operate in relativistic jets: (i) internal shocks forming between jet portions moving at different velocities (e.g., Spada et al. 2001); (ii) external (oblique/reconfinement) shocks which mediate the pressure balance between jets and their environment (e.g., Komissarov 1994; Bromberg & Levinson 2009; Nalewajko & Sikora 2009); and magnetic reconnection, formed on global scales in the case of jets with alternating currents (e.g., Lovelace et al. 1997; Giannios, & Uzdensky 2019), or driven by turbulence in magnetised plasma¹ (see Comisso, & Sironi 2019; Zhdankin et al. 2020; Sobacchi, & Lyubarsky 2019, and refs. therein). Discriminating between these potential dissipation processes is complicated by the fact that all of them tend to bring the dissipated plasma closer to equipartition between the magnetic and internal energy densities (Sironi et al. 2015). Should the energy density of the jet plasma be dominated by the electron-positron pairs (see §2.1), reconnection would be the favoured dissipation mechanism, since in that case the dissipated energy is shared roughly evenly between all particles (Petropoulou et al. 2019).

4 DISCUSSION

According to the most popular model of relativistic jets, they are launched dominated by the Poynting flux, and are gradually converted become dominated by the cold protons (for review, see Blandford et al. 2019, and refs. therein). The kinetic energy of cold protons would be further dissipated in the terminal shocks, and converted to relativistically hot protons and ultra-relativistic electron-positron pairs. Prior to the terminal shocks, the jet magnetic fields are expected to be dominated by the toroidal component, and hence such shocks are predicted to be ‘perpendicular’. Recent PIC simulations of perpendicular shocks indicate that acceleration of electrons/positrons in such shocks is very inefficient, and

most of the energy of such cold jets would be converted to the internal energy of the protons (Sironi & Spitkovsky 2011; Crumley et al. 2019). This seems to be challenged by detailed studies of the radio lobes, which indicate that at least half of their internal energy is contributed by the relativistic pairs (Snios et al. 2018, and refs. therein). This problem can be overcome by assuming that in the large-scale jets the dominant portion of the energy flux is carried by relativistically hot pairs.

As we demonstrated in §2.1, such a picture of relativistic jets is supported by a combination of observational data on radio lobes and blazars. Their pair contents are $n_e/n_p \sim 20$, and average energies of leptons and protons are $\bar{\gamma}_e \sim 100$ and $\bar{\gamma}_p < 2$, respectively. While the pair content is likely to be established already at the jet base, where pairs can be created by high energy photons produced in accretion disk corona (see §3.1.1), it is not clear whether loading by protons, at the estimated rate of $\sim 1\%$ of the accretion rate, can be achieved also at the jet base – by interchange instabilities developed between the accretion flow and the electromagnetic outflow, or are dominated by such processes working on larger scales, like stellar winds (see §3.1.2).

The proposed scenario of relativistic jets dominated in terms of particle numbers by the e^+e^- pairs is supported independently by the studies of blazars and radio lobes. In order for the jets to be dominated by pairs also in terms of energy flux, it is required that dissipative mechanisms maintain the pairs at the average random Lorentz factor of $\bar{\gamma}_e \gtrsim (n_p m_p)/(n_e m_e) \sim 100(20n_p/n_e)$. At distance scales larger than tens of parsecs, the radiative cooling of even ultra-relativistic electrons is inefficient, and in order to maintain the energy flux of pairs, the required heating rate is determined mainly by the need to compensate the adiabatic losses (Potter, & Cotter 2015; Zdziarski et al. 2019). Such heating can be mediated by the oblique/reconfinement shocks, which regulate the pressure balance between the jet and its environment, and are predicted to stimulate the kink instabilities followed by a variety of particle acceleration mechanisms (e.g., Tchekhovskoy, & Bromberg 2016; Barniol Duran et al. 2017; Alves et al. 2018; Das, & Begelman 2019). Since the formation of such shocks requires the upstream flow to be supersonic, we can expect them to become weaker when the energy flux carried by the pairs starts to dominate over the energy flux carried by the ‘cold’ protons.

One can also consider a scenario where due to rapid lateral expansion and efficient adiabatic losses, e.g. in the ‘conical’ jet zone, we would locally have $P_{e,\text{jet}} \ll P_{p,\text{jet}}$, in which case the jets would be supersonic even relative to surfaces with small opening angles, and the pressure balance between the jet and its environment would involve the formation of reconfinement shocks. This would be followed by efficient heating of the jet plasma, which would eventually result in $P_{e,\text{jet}} \sim P_{p,\text{jet}}$, at which point the reconfinement shocks would become very weak (e.g., Daly & Marscher 1988).

The dissipative processes can work efficiently within the host galaxy (in the ‘conical’ jet zone), where the jet is expanding due to the external pressure decreasing strongly with the distance. At some point the external support becomes provided by the cocoon made of the shocked jet plasma. Due to the fact that the age of the typical FR II sources significantly exceeds their sound-crossing time scale,

¹ In relativistic jets, turbulence can be sustained by a variety of instabilities developing in the presence of toroidal magnetic fields (e.g., Begelman 1998; Alves et al. 2018; Bromberg et al. 2019), shear layers (for recent review, see Rieger 2019), or recollimation shock waves (e.g., Gourgoullias, & Komissarov 2018), but also due to interactions of the jet with ‘internal’ obstacles (dense molecular clouds and/or Wolf-Rayet stars with strong winds; see, e.g., Perucho 2019).

the external pressure provided by the cocoon is roughly uniform. This implies that large-scale jets are approximately ‘cylindrical’, and therefore such hot jets may survive up to the terminal shocks without significant energy losses (see, e.g., Bromberg et al. 2011).

Using our premise that the dissipative mechanisms operating in the FR II jets tend to maintain $P_{e,\text{jet}} \gtrsim P_{p,\text{jet}}$ could shed light on the origin of the FR dichotomy of radio galaxies (Fanaroff & Riley 1974; Mingo et al. 2019). Since the FR I jets are in general less powerful, loading them with the protons can be expected to be relatively more efficient, either intrinsically by the stellar winds (Komissarov 1994; Perucho et al. 2014), or externally due to interchange or Kelvin-Helmholtz instabilities (e.g., Rossi et al. 2008). Hence, the FR I jets are expected to be characterised by $n_e/n_p \ll 20$. Furthermore, the $P_{e,\text{jet}} \sim P_{p,\text{jet}}$ relation implies also that $\bar{\gamma}_{e,\text{jet}} \propto n_p/n_e$, and hence the stronger baryonic loading of the FR I jets could explain why the synchrotron spectra of the large-scale FR I jets indicate larger values of $\bar{\gamma}_{e,\text{jet}}$ than in FR II objects (e.g., Dulwich et al. 2007; Hardcastle et al. 2007; Worrall 2009; Harris et al. 2009).

5 SUMMARY

The energetic dominance of electron-positron pairs over protons in the radio lobes of luminous FR II radio galaxies and quasars — suggested by observations — would be very difficult to achieve if the radio lobes were inflated by jets dominated by cold protons. Therefore, we adopted an idea that relativistically hot pair plasma is the main component of relativistic jets on large scales (Snios et al. 2018). Assuming that the energy division between protons, leptons and magnetic fields is the same in the jets as in the lobes, we obtain an estimate of the pair content in the large-scale FR II jets ($n_e/n_p \sim 20$) that is consistent with previous estimates for the small-scale jets based on modelling the SEDs and the energetics of blazars (e.g., Sikora et al. 2013; Pjanka et al. 2017). We also estimate the average electron energy in the FR II jets as $\bar{\gamma}_{e,\text{jet}} \sim 100$.

Once the jets become loaded with pairs (intrinsically by means of photon-photon pair production) and with protons (externally by means of various boundary instabilities, or intrinsically due to stellar winds), once they become bulk accelerated, dominated energetically by relativistically hot leptons and trans-relativistic protons, and radiatively inefficient, it should not be difficult to maintain them in such a state up to the terminal shocks.

In the case of low-power FR I jets and associated with them BL Lac type blazars, we suggest that loading them with protons should be more efficient than loading with pairs, and hence in that case we expect $n_e \sim n_p$. This difference in the jet composition could explain the higher values of $\bar{\gamma}_{e,\text{jet}}$ inferred observationally in large-scale FR I jets.

ACKNOWLEDGEMENTS

We thank the Reviewer for helpful suggestions. We acknowledge financial support by the Polish National Science Centre grants 2016/21/B/ST9/01620 and 2015/18/E/ST9/00580.

REFERENCES

- Abdo, A. A., Ackermann, M., Ajello, M., et al. 2011, *ApJ*, 733, L26
- Ackermann, M., Anantua, R., Asano, K., et al. 2016, *ApJ*, 824, L20
- Aharonian, F. A. 2002, *MNRAS*, 332, 215
- Algaba, J. C., Nakamura, M., Asada, K., et al. 2017, *ApJ*, 834, 65
- Alves, E. P., Zrake, J., & Fiuza, F. 2018, *Phys. Rev. Lett.*, 121, 245101
- Barniol Duran, R., Tchekhovskoy, A., & Giannios, D. 2017, *MNRAS*, 469, 4957
- Bassani, L., Venturi, T., Molina, M., et al. 2016, *MNRAS*, 461, 3165
- Begelman, M. C., & Li, Z.-Y. 1994, *ApJ*, 426, 269
- Begelman, M. C., 1998, *ApJ*, 493, 291
- Beloborodov, A. M. 1999, *MNRAS*, 305, 181
- Beskin, V. S., & Nokhrina, E. E. 2006, *MNRAS*, 367, 375
- Blandford, R. D., & Znajek, R. L. 1977, *MNRAS*, 179, 433
- Blandford, R., Meier, D., & Readhead, A. 2019, *ARA&A*, 57, 467
- Bogovalov, S., & Tsiganos, K. 2005, *MNRAS*, 357, 918
- Böttcher, M., Reimer, A., Sweeney, K., et al. 2013, *ApJ*, 768, 54
- Bromberg, O., & Levinson, A., 2009, *ApJ*, 699, 1274
- Bromberg, O., Nakar, E., Piran, T., et al. 2011, *ApJ*, 740, 100
- Bromberg, O., Singh, C. B., Davelaar, J., et al. 2019, *ApJ*, 884, 39
- Burlon, D., Ghirlanda, G., Murphy, T., et al. 2013, *MNRAS*, 431, 2471
- Carilli, C. L., Perley, R. A., Dreher, J. W., et al. 1991, *ApJ*, 383, 554
- Cavagnolo, K. W., McNamara, B. R., Nulsen, P. E. J., et al. 2010, *ApJ*, 720, 1066
- Chatterjee, K., Liska, M., Tchekhovskoy, A., et al. 2019, *MNRAS*, 490, 2200
- Comisso, L., & Sironi, L. 2019, *ApJ*, 886, 122
- Croston, J. H., Hardcastle, M. J., Harris, D. E., et al. 2005, *ApJ*, 626, 733
- Croston, J. H., Ineson, J., & Hardcastle, M. J. 2018, *MNRAS*, 476, 1614
- Crumley, P., Caprioli, D., Markoff, S., et al. 2019, *MNRAS*, 485, 5105
- Daly, R. A., & Marscher, A. P. 1988, *ApJ*, 334, 539
- Das, U., & Begelman, M. C. 2019, *MNRAS*, 482, 2107
- Dulwich, F., Worrall, D. M., Birkinshaw, M., et al. 2007, *MNRAS*, 374, 1216
- Falle, S. A. E. G. 1991, *MNRAS*, 250, 581
- Fan, X.-L., Wu, Q., & Liao, N.-H. 2018, *ApJ*, 861, 97
- Fanaroff, B. L., & Riley, J. M., 1974, *MNRAS*, 167, 31P
- Fernandes, C. A. C., Jarvis, M. J., Rawlings, S., et al. 2011, *MNRAS*, 411, 1909
- Ghisellini, G., Tavecchio, F., Maraschi, L., et al. 2014, *Nature*, 515, 376
- Giannios, D., & Uzdensky, D. A. 2019, *MNRAS*, 484, 1378
- Godfrey, L. E. H., Bicknell, G. V., Lovell, J. E. J., et al. 2009, *ApJ*, 695, 707
- Godfrey, L. E. H., Lovell, J. E. J., Burke-Spolaor, S., et al. 2012, *ApJ*, 758, L27
- Godfrey, L. E. H., & Shabala, S. S. 2013, *ApJ*, 767, 12
- Gondek, D., Zdziarski, A. A., Johnson, W. N., et al. 1996, *MNRAS*, 282, 646
- Gourgouliatos, K. N., & Komissarov, S. S. 2018, *Nature Astronomy*, 2, 167
- Gupta, M., Sikora, M., Rusinek, K., & Madejski, G. M. 2018, *MNRAS*, 480, 2861
- Hardcastle, M. J., Kraft, R. P., Sivakoff, G. R., et al. 2007, *ApJ*, 670, L81
- Hardcastle, M. J. 2018, *MNRAS*, 475, 2768

- Harris, D. E., Cheung, C. C., Stawarz, L., et al. 2009, *ApJ*, 699, 305
- Harris, D. E., Moldón, J., Oonk, J. R. R., et al. 2019, *ApJ*, 873, 21
- Ineson, J., Croston, J. H., Hardcastle, M. J., et al. 2017, *MNRAS*, 467, 1586
- Janiak, M., Sikora, M., & Moderski, R. 2015, *MNRAS*, 449, 431
- Kang, S.-J., Chen, L., & Wu, Q. 2014, *ApJS*, 215, 5
- Kataoka, J., & Stawarz, L. 2005, *ApJ*, 622, 797
- Kawakatu, N., Kino, M., & Takahara, F. 2016, *MNRAS*, 457, 1124
- Kino, M., Kawakatu, N., & Takahara, F. 2012, *ApJ*, 751, 101
- Komissarov, S. S. 1994, *MNRAS*, 269, 394
- Lovelace, R. V. E., Newman, W. I., & Romanova, M. M., 1997, *ApJ*, 484, 628
- Lyubarsky, Y. 2009, *ApJ*, 698, 1570
- Lyubarsky, Y. E. 2010, *MNRAS*, 402, 353
- Madejski, G. M., & Sikora, M. 2016, *ARA&A*, 54, 725
- McKinney, J. C., Tchekhovskoy, A., & Blandford, R. D. 2012, *MNRAS*, 423, 3083
- Mignone, A., Rossi, P., Bodo, G., et al. 2010, *MNRAS*, 402, 7
- Mingo, B., Croston, J. H., Hardcastle, M. J., et al. 2019, *MNRAS*, 488, 2701
- Murase, K., Inoue, Y., & Dermer, C. D. 2014, *Phys. Rev. D*, 90, 023007
- Nakamura, M., & Asada, K. 2013, *ApJ*, 775, 118
- Nalewajko, K., Sikora, M., 2009, *MNRAS*, 392, 1205
- Nalewajko, K., Begelman, M. C., & Sikora, M. 2014, *ApJ*, 789, 161
- Narayan, R., Igumenshchev, I. V., & Abramowicz, M. A. 2003, *PASJ*, 55, L69
- O’ Riordan, M., Pe’er, A., & McKinney, J. C. 2018, *ApJ*, 853, 44
- Panessa, F., Tarchi, A., Castangia, P., et al. 2015, *MNRAS*, 447, 1289
- Perlman, E., Meyer, E., Eilek, J., et al. 2019, *BAAS*, 51, 59
- Perucho, M., Martí, J. M., Laing, R. A., et al. 2014, *MNRAS*, 441, 1488
- Perucho, M. 2019, *Galaxies*, 7, 70
- Petropoulou, M., Sironi, L., Spitkovsky, A., et al. 2019, *ApJ*, 880, 37
- Pjanka, P., Zdziarski, A. A., & Sikora, M. 2017, *MNRAS*, 465, 3506
- Potter, W. J., & Cotter, G. 2015, *MNRAS*, 453, 4070
- Punsly, B. 2007, *MNRAS*, 374, L10
- Punsly, B., Igumenshchev, I. V., & Hirose, S. 2009, *ApJ*, 704, 1065
- Rawlings, S., & Saunders, R. 1991, *Nature*, 349, 138
- Ricci, C., Trakhtenbrot, B., Koss, M. J., et al. 2017, *ApJS*, 233, 17
- Rieger, F. M. 2019, *Galaxies*, 7, 78
- Rodrigues, X., Fedynitch, A., Gao, S., et al. 2018, *ApJ*, 854, 54
- Rossi, P., Mignone, A., Bodo, G., et al. 2008, *A&A*, 488, 795
- Rusinek, K., Sikora, M., Koziel-Wierzbowska, D., et al. 2017, *MNRAS*, 466, 2294
- Shabala, S. S., & Godfrey, L. E. H. 2013, *ApJ*, 769, 129
- Sikora, M., Stawarz, L., Moderski, R., et al. 2009, *ApJ*, 704, 38
- Sikora, M., Janiak, M., Nalewajko, K., et al. 2013, *ApJ*, 779, 68
- Sikora, M. 2016, *Galaxies*, 4, 12
- Sironi, L., & Spitkovsky, A., 2011, *ApJ*, 726, 75
- Sironi, L., Petropoulou, M., & Giannios, D. 2015, *MNRAS*, 450, 183
- Snios, B., Nulsen, P. E. J., Wise, M. W., et al. 2018, *ApJ*, 855, 71
- Sobacchi, E., & Lyubarsky, Y. E. 2019, *MNRAS*, 2965
- Spada, M., Ghisellini, G., Lazzati, D., & Celotti, A., 2001, *MNRAS*, 325, 1559
- Stawarz, L., Cheung, C. C., Harris, D. E., et al. 2007, *ApJ*, 662, 213
- Tavecchio, F., Cerutti, R., Maraschi, L., et al. 2005, *ApJ*, 630, 721
- Tchekhovskoy, A., Narayan, R., McKinney, J. C., 2011, *MNRAS*, 418, L79
- Tchekhovskoy, A., & Bromberg, O. 2016, *MNRAS*, 461, L46
- Turner, R. J., Shabala, S. S., & Krause, M. G. H. 2018, *MNRAS*, 474, 3361
- Vila, G. S., Vieyro, F. L., & Romero, G. E. 2014, *International Journal of Modern Physics Conference Series*, 1460191
- Willott, C. J., Rawlings, S., Blundell, K. M., et al. 1999, *MNRAS*, 309, 1017
- Worrall, D. M. 2009, *A&ARv*, 17, 1
- Zakamska, N. L., Begelman, M. C., & Blandford, R. D. 2008, *ApJ*, 679, 990
- Zdziarski, A. A., & Bottcher, M. 2015, *MNRAS*, 450, L21
- Zdziarski, A. A., Stawarz, L., & Sikora, M. 2019, *MNRAS*, 485, 1210
- Zhdankin, V., Uzdensky, D. A., Werner, G. R., et al. 2020, *MNRAS*, doi:10.1093/mnras/staa284